nature physics

ARTICLES

PUBLISHED ONLINE: 2 FEBRUARY 2015 | DOI: 10.1038/NPHYS3186

Experimental realization of long-distance entanglement between spins in antiferromagnetic quantum spin chains

S. Sahling[1,2,3], G. Remenyi[1,2], C. Paulsen[1,2], P. Monceau[1,2], V. Saligrama[4], C. Marin[4], A. Revcolevschi[5], L. P. Regnault[6], S. Raymond[6] and J. E. Lorenzo[1,2]*

Entanglement is a concept that has defied common sense since the discovery of quantum mechanics. Two particles are said to be entangled when the quantum state of each particle cannot be described independently, no matter how far apart in space and time the two particles are. We demonstrate experimentally that unpaired spins separated by several hundred ångström entangle through a collection of spin singlets made up of antiferromagnetic spin-1/2 chains in a bulk material. Low-temperature magnetization and specific heat studies as a function of magnetic field reveal the occurrence of very dilute spin dimers and at least two quantum phase transitions related to the breaking of excited local triplets. The mechanism at the origin of the unpaired spins inside the quantum chains is the inter-modulation potential between two sublattices, and may be replicated using well-designed synthetic multilayers.

Entanglement is an essential feature of the macroscopic world[1], despite the fact that human perception has difficulty accepting such strange predictions. A very fruitful area of research today is quantum computing technology, where entanglement is being harnessed for eventual use in quantum computation and communications[2,3]. Scientists are also developing new areas of research where entanglement could lie at the origin of the interactions in ever larger objects, ranging from photons to clusters of atoms to molecules—and even to cosmological objects.

Most of the protocols for quantum communication rely on entangled photons[4], as they are weakly interacting and can be easily manipulated using existing optical fibre technology. However, it is not always convenient to use photons to exchange information as, in particular, it is not straightforward to convert information between physically different qubits. Another approach described in seminal papers by Bose[5,6] suggested the use of spin chains as quantum channels for short- or mid-range communication, showing that, by means of the magnetic interaction between the spins that compose the chain, the transfer of information arises naturally as the system evolves dynamically, without the requirement for any external control. Transferring quantum information between distant qubits through spin chains would be highly desirable. However, this procedure often requires the repeated application of swapping gates and is, consequently, very demanding experimentally. Moreover, the features that characterize the transmission, such as teleportation, fidelity, transfer quality and speed, depend on the properties of the underlying quantum system[2,3].

Other developments have explored the conditions for long-distance entanglement without the need to perform operations and measurements. Among the many possible spin configurations it seems that antiferromagnetic spin arrays characterized by spin gaps above the ground state can exhibit true entanglement over long distances[7]. Furthermore, the entanglement is a slowly decreasing function of distance, allowing robust teleportation across finite distances[8]. Figure 1 sketches the components required to give long-distance entanglement of unpaired spins S_A and S_B in a gapped spin-chain system. (Note that long-distance entanglement in gapless spin chains has also been predicted and studied in detail, and its features are captured well by two-impurity Kondo physics[5,9,10].)

In this paper we present the first example of a bulk material, made up of dimerized spin-1/2 chains, where single spins approximately 220–250 Å apart become entangled through a chain of spin dimers below ≈2.1 K. The key feature of $Sr_{14}Cu_{24}O_{41}$ is that it is a composite layered structure made up of alternating spin-ladder sublattice layers and spin-chain sublattice layers, in such a way that, along the chain (and ladder) axis of both subsystems, the structure is near commensurate in the ratio $c_c/c_l \approx 10/7$ (Supplementary Methods for more details)[11]. As discussed by Gellé and Lepetit[12], the variation of the modulation potential of the ladders onto the chains singles out special sites in the chain that favour the occurrence of unpaired spins into an otherwise uniform spin-dimer chain. The number of unpaired spins calculated using this model is of the order of 1 in 20 Cu atoms in the chain. Results from inelastic neutron scattering[13,14] are compatible with an almost uniform arrangement of spin dimers (Supplementary Methods), and previous low-temperature magnetization studies[15] have stressed the presence of at most 1% of unpaired spins.

Figure 1a shows how the transmission protocol between spins at sites A and B takes place by way of a spin channel. Although S_A and S_B do not interact directly they experience an effective interaction through the spin chain. The Hamiltonian that describes the entanglement between S_A and S_B can be written as

$$H = J_p\,(S_A \cdot S_1 + S_B \cdot S_N) + H_C \qquad (1)$$

[1]Université Grenoble Alpes, Institut Néel, F-38042 Grenoble, France. [2]CNRS, Institut Néel, F-38042 Grenoble, France. [3]TU Dresden, Institut für Festkörperphysik, D-01062, Germany. [4]SPSMS, UMR-E 9001, CEA-INAC/UJF-Grenoble 1, IMAPEC, F-38054 Grenoble, France. [5]Synthèse, Propriétés et Modélisation des Matériaux (SP2M), UMR 8182, Université Paris-Sud, 91405 Orsay Cedex, France. [6]SPSMS-MDN, UMR-E 9001, CEA/UJF-Grenoble 1, INAC, F-38054 Grenoble, France. *e-mail: emilio.lorenzo@neel.cnrs.fr

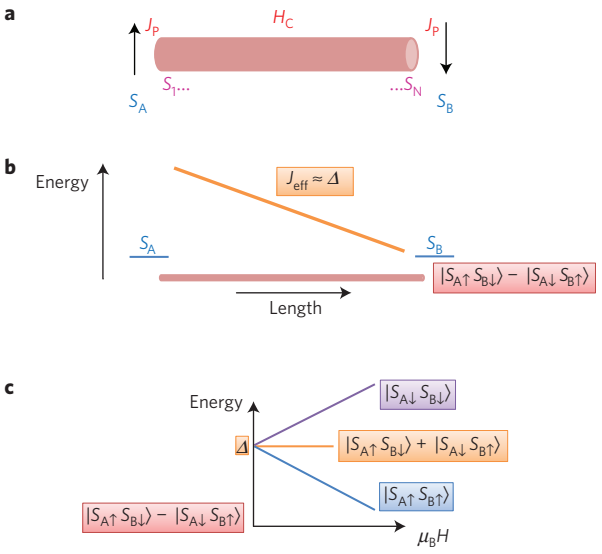

Figure 1 | Sketch of a quantum communication channel and properties of spins entangled through antiferromagnetic interactions. a, Spins S_A and S_B are entangled through a spin chain C of length L. J_p is the spin exchange between spins at S_A and S_B and the chain. H_C is the Hamiltonian of the spin chains. **b**, Sketch of the variation of the energy gap, Δ, as a function of the length L in a log–log plot. Δ is proportional to the effective spin exchange between S_A and S_B and to the spin exchange constant of H_C renormalized by the length L (or the number of sites in L). As a result, S_A and S_B form an antiferromagnetic entangled state with a ground state (singlet) that is expressed as $|S_{A\uparrow}S_{B\downarrow}\rangle - |S_{A\downarrow}S_{B\uparrow}\rangle$. **c**, The spin triplet splits on application of a magnetic field following the Zeeman relation: $\Delta(H) = \Delta(0) \pm g\mu_B H$ for $|S_{A\uparrow}S_{B\uparrow}\rangle$ and $|S_{A\downarrow}S_{B\downarrow}\rangle$; $\Delta(H) = \Delta(0)$ for $|S_{A\uparrow}S_{B\downarrow}\rangle + |S_{A\downarrow}S_{B\uparrow}\rangle$.

J_p is the exchange constant between spins S_A (and S_B) and the chain, S_1 and S_N are the end spins of the spin chain and H_C is the spin-chain Hamiltonian,

$$H_C = \sum_{i=1}^{N} (J_1 S_{2i} \cdot S_{2i+1} + J_2 S_{2i} \cdot S_{2i-1}) \qquad (2)$$

where the sum in i is over the N active Cu-sites, (which is four in a formula unit of a length of 27.5 Å, see filled blue circles in Fig. 2). It has been established that $J_1 \approx 115$ K and $J_2 \approx -13$ K (ferromagnetic) in $Sr_{14}Cu_{24}O_{41}$ (refs 13,14), which gives rise to a pattern of up–up–down–down spins along the chain. The magnitude of J_p is difficult to calculate from first principles in view of the large variation of Cu–O bond distances and Cu–O–Cu bond angles in the incommensurate chain. To a first approximation, and whenever the scheme in Fig. 2c is valid[12], $J_p \approx J_2$. The interchain interaction, $J_\perp < J_1/5$ is antiferromagnetic, can be neglected in the formation of next-nearest neighbour spin dimers along the chain axis. However, it can not be neglected in the formation of long-distance dimers as it gives rise to extra paths for spin entanglement.

Because of the rotational invariance, and assuming that $J_p/J_1 \ll 1$, equation (2) can be effectively mapped onto an SU(2)-symmetric Hamiltonian for the sites A and B:

$$H_{eff} = J_{eff} S_A \cdot S_B \qquad (3)$$

J_{eff} is just the spin singlet-to-triplet gap, Δ, which according to conformal field theory[16] scales as $\approx (J_1 + J_2)/2N$ (Fig. 1b). In other words if the spin chain includes $10(J_1 - J_2)$ units the effective exchange will become of the order of a few kelvin. Quite generally it has been seen that the magnitude (and sign) of J_p also plays a role by renormalizing the exponent: $J_{eff} \propto N^{-\alpha}$ (ref. 8). $\alpha = 1$ for $J_p/J_1 = -0.2$ (and J_p ferromagnetic) and $\alpha = 0.2$ for $J_p/J_1 = 0.2$ (and J_p antiferromagnetic).

If spins S_A and S_B are to be used for quantum information in the spin channel, it is necessary to show that both spin states are entangled. Alternating antiferromagnetic spin 1/2 chains and ladders exhibit spin dimers as the ground state. In particular, $Cu(NO_3)_2 \cdot 2.5D_2O$ and $NH_4CuPO_4 \cdot H_2O$ have been used to quantify entanglement by using magnetic susceptibility[17–21] and heat capacity[19,22–24] as entanglement witnesses. Another way to detect entanglement is to induce a quantum phase transition by, for instance, the application of a magnetic field, as sketched in Fig. 1c. One of the components of the triplet mixes with the ground state singlet, the entangled state de-coheres and the entanglement decays analytically on approaching the critical magnetic field[21,25,26]. Beyond that critical field the magnetization and specific heat dependences with temperature follow the known laws for unpaired spins (Supplementary Methods).

With this objective, ultralow-temperature magnetization and specific heat experiments under a magnetic field were performed. Experiments using inelastic neutron scattering at 60 mK have also been carried out, but no trace of the spin structure or associated excitations was observed. This is not surprising in view of the small number of unpaired spins and, therefore, of the very small scattering cross-section of these excitations.

Magnetization experiments as a function of temperature and magnetic field were performed on two samples of $Sr_{14}Cu_{24}O_{41}$ of different origin and are shown in Fig. 3, where the field direction was along the c-axis. In a small field of 0.1 T the magnetization as a function of temperature reaches a maximum at around 1.3 K, and then diverges as $\approx 1/T$ as $T \to 0$. In Fig. 3a the ultralow-temperature magnetization data have been fitted with a Curie law which accounts for the low-temperature divergence of a small population of unpaired free spins. More interestingly, the broad maxima is fitted with the formula for antiferromagnetic spin dimers, yielding a gap $\Delta = 2.3$ K. This represents a fourth category of spin dimer present in $Sr_{14}Cu_{24}O_{41}$, and is distinguished from the others by its small energy gap. In contrast, the other three types of dimers form at temperatures orders of magnitude higher and are essentially frozen at low temperature. Specifically they are the Zhang–Rice singlet (white circles in Fig. 2), with $\Delta_{ZR} \approx 5{,}000$–$15{,}000$ K (ref. 27), the spin-ladder sublattice, with $\Delta_{ladder} \approx 350$ K (refs 28,29), and the spin-chain sublattice, with $\Delta_{chain} \approx 115$ K (refs 13,14).

Magnetization experiments as a function of the magnetic field (Fig. 3b for sample 2 and Fig. 3c for sample 1) show the occurrence of three magnetization plateaux developing below 500 mK: one due to the unpaired free spins at $M_{p0} = 0.00123(5)\mu_B$/Cu and two others developing above 2 and 3 T, at $M_{p1} = 0.0054(1)\mu_B$/Cu and $M_{p2} = 0.0020(1)\mu_B$/Cu, respectively. Similar behaviour was found when the field was applied along the b-axis. (Supplementary Methods). The $M(H)$ data were analysed using the Brillouin function for the unpaired free spins which describes the first plateau. The other plateaux are fitted with the dimer model, using a field-dependent gap according to the Zeeman splitting for a triplet, $\Delta(H) = \Delta - g\mu_B H/k_B$. Therefore, the critical field is proportional to the spin singlet-to-triplet gap. For the first group of dimers we found $\mu_0 H_{c1} = 1.53$ T ($\| c$), which according to the Zeeman splitting for $S = 1/2$ dimers, gives a value for the gap of $\Delta_1 = 2.27$ K, in excellent agreement with the value deduced from the fit of the magnetization versus temperature data shown in Fig. 3a. If we assume that the second group of spins at the origin of M_{p2} are also dimers, we found $\mu_0 H_{c2} \approx 2.4$ T and the extracted gap is $\Delta_2 \approx 3.6$ K. The first gap is reproducible between the two samples, with very similar M_{p1} values for each sample. Unfortunately, this is not the case for the second gap, with very different critical field and magnetization values. Magnetization experiments as a function of temperature were carried out for sample 1 (Fig. 3c) and agree with

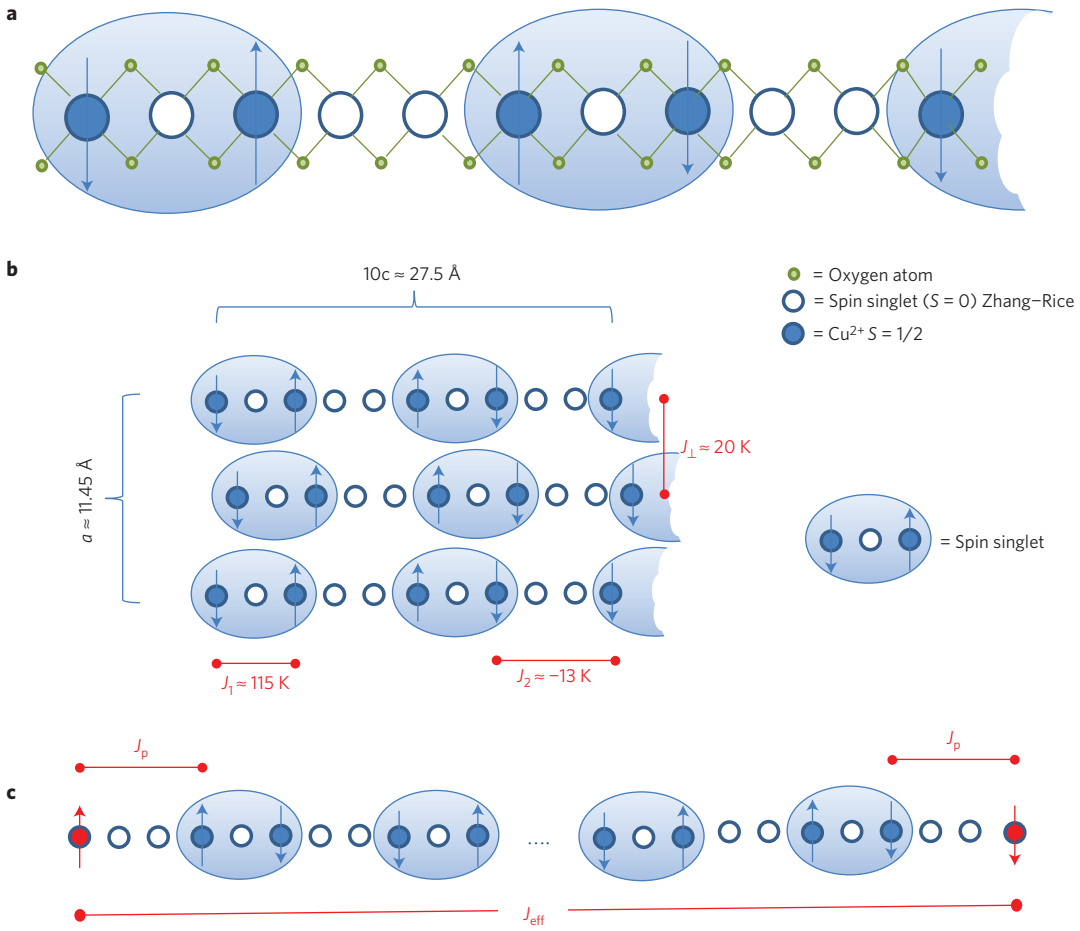

Figure 2 | Detailed description of the structure and magnetic properties of the chain subsystem. a, Pattern of spin dimers and Zhang–Rice singlets (representing an effective Cu^{3+}) in the chain sublattice as deduced from inelastic neutron scattering[14]. Filled circles are Cu^{2+} with spin $S=1/2$. Open circles are Zhang–Rice singlets with a total spin $S=0$, arising from the coupling between the spin of an extra-hole and a Cu^{2+} $S=1/2$. It is assumed that there are no holes in the ladder sublattice. It should be noted that all these spins dimers (either the Zhang–Rice or the next-nearest neighbour Cu^{2+}) are entangled states with a ground state represented by $|S_{1\uparrow}S_{2\downarrow}\rangle - |S_{1\downarrow}S_{2\uparrow}\rangle$. **b**, $Sr_{14}Cu_{24}O_{41}$ unit cell in the *ac*-plane, showing the chains sublattice. Included are the lattice parameters, and the magnetic exchange constants deduced from inelastic neutron scattering[13,14]. **c**, Spin-dimer chains with single spins (in red), as proposed by *ab initio* calculations[12]. The effective spin exchange, J_{eff}, between isolated spins (separated by a distance L) is of the order of a few kelvin.

the temperature dependence that can be extracted from the above-mentioned model (Fig. 3d).

Specific heat experiments were carried out as a function of temperature (down to 80 mK) and magnetic field (up to 10 T). The same sample as in the magnetization studies in Fig. 3, sample 2, was used in these experiments and the applied magnetic field was along the *c*-direction. The results are shown in Fig. 4. Details of the experimental method can be found in the Supplementary Methods. Two features appear above the baseline of non-magnetic excitations (dash-dotted line in Fig. 4a). First, a hump centred at around 1 K and, second, an upturn that strongly depends on the value of the magnetic field. A fit of the data shows again that the hump can be attributed to gapped excitations of magnetic origin. The fit shown in the figure uses an equation for a chain of spin dimers with a single gap[22,30,31], $C_P(\beta) \approx (\Delta\beta)^{1.5}\exp(-\Delta\beta)$, where $\beta = 1/k_B T$, and not surprisingly becomes even better using two or three gaps. The ultralow-temperature upturns for all three magnetic fields in Fig. 4b are well accounted for by a Schottky contribution, $C_P(\theta,\beta) \approx N_{fs}\,(\theta\beta)^2\,e^{-\theta\beta}/(1+e^{-\theta\beta})^2$, and $\theta = 2\mu_B H$, where the global amplitude, N_{fs}, is the only fitting parameter for all three curves. This Schottky contribution is analogous to the contribution of unpaired free spins seen in magnetization experiments that was characterized by the Curie and Brillouin laws. The intermediate magnetic fields, between 0.6 and 3 T, exhibit a great complexity, which is beyond the scope of this paper. Indeed, in addition to the magnetic part there are further contributions from a charge density wave, making a complete and accurate analysis of the specific heat as a function of the magnetic field rather challenging.

Both low-temperature magnetization and specific heat experiments have revealed the same features for two different samples: the presence of a very dilute population of unpaired free spins ($\approx 10^{-3}$/Cu), which remain free down to the lowest temperature measured, and a slightly larger population of unpaired spins (≈ 2–2.5×10^{-3}/Cu), which couple antiferromagnetically to form dimers at low temperature with spin singlet-to-triplet gaps of 2.3 and 3.6 K, respectively. Where do these dimers come from? We can eliminate an extrinsic impurity origin as: no traces belonging to any other phase have been found in the powder X-ray diffraction experiments and all the diffraction peaks can be indexed within the $Sr_{14}Cu_{24}O_{41}$ structure; experiments have been carried out on two samples of different origin and our results regarding the number of unpaired spins above 1 K (Fig. 3b) are in good agreement with published data[32,33]; and the characteristic spin exchange energies, a few kelvin, are very small compared to those of analogous exchange constants in spin systems exhibiting CuO_2 chains[34]. Moreover the observed features correspond to well-defined energies and

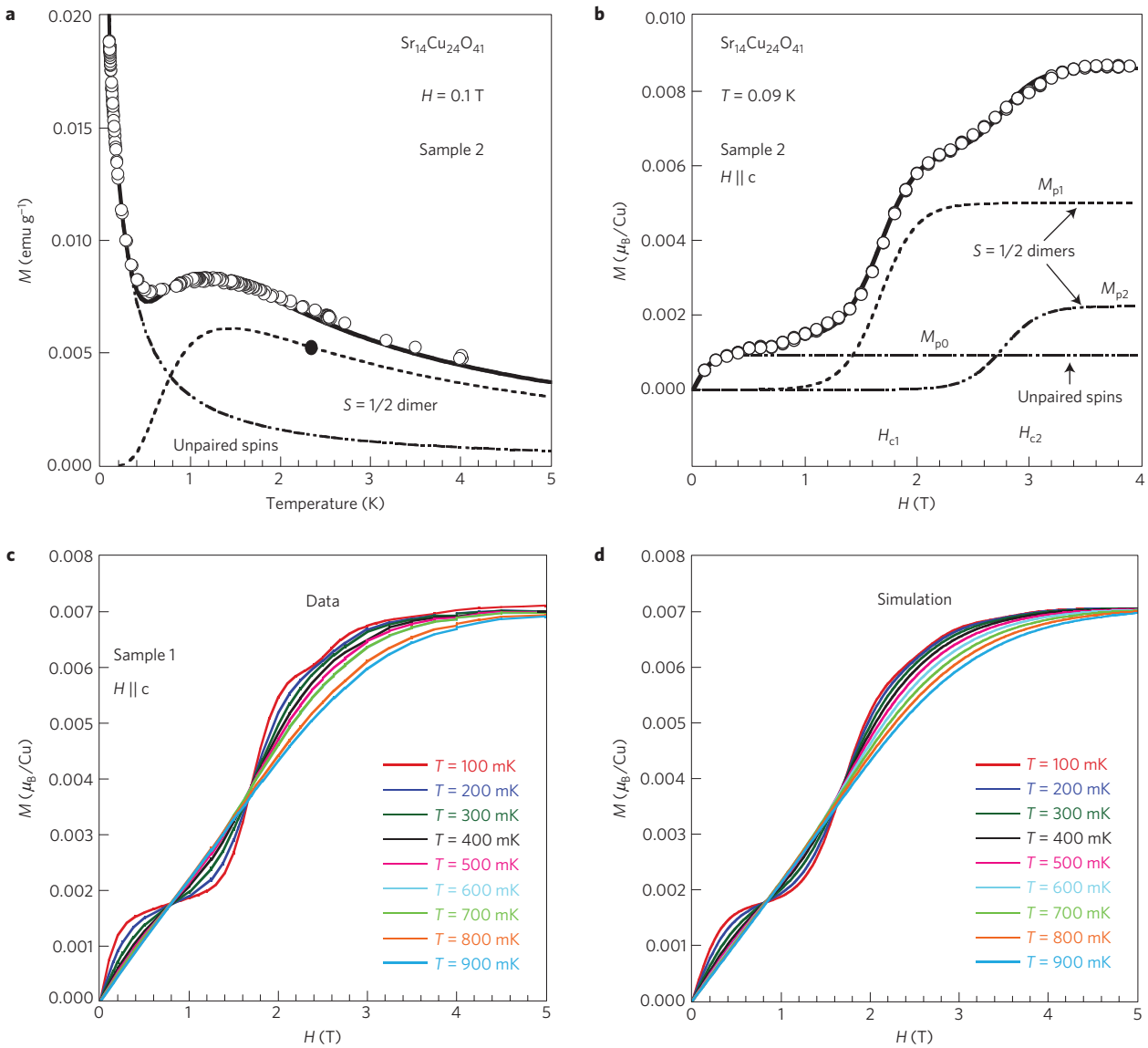

Figure 3 | Magnetization data at low temperature and under magnetic fields. a, Magnetization as a function of temperature for temperatures below 5 K. Two features are evident: a maximum at 1.3 K, which we interpret as arising from the formation of spin dimers between distant unpaired spins with a spin singlet-to-triplet gap of $\Delta_1 \approx 2.3$ K (red point), and a rapid uprise below 1 K, which we interpret as being due to a small concentration of unpaired spins that remain free down to our lowest temperature. Dash and dash-dotted lines represent the fit with the corresponding equations (Supplementary Methods). **b**, Magnetic field dependence of the magnetization at the lowest measured temperature, 90 mK. Data were analysed with three components: a Brillouin function describing the magnetization of unpaired spins and two dimer contributions with the gap linearly depending on the magnetization (Zeeman effect). The gaps deduced for the two spin-1/2 dimers, following the Zeeman splitting ($\Delta = g\mu_B H_C/k_B$), are $\Delta_1 \approx 2.3$ K and $\Delta_2 \approx 3.6$ K. **c**, Magnetic field dependence of the magnetization for nine temperatures below 1 K for sample 1. **d**, Simulation of the data in **c** using the data analysis described in the Supplementary Methods. The simulation was performed by fitting the low-temperature data, then fixing the parameters and applying only the temperature variation of equations.

magnetic fields and not to a distribution of energies, as one would expect for an extrinsic origin. By using analogous arguments we can rule out impurities in the form of trimers or, in general, multimers being formed. Or, if there are any, they are very few in number and their characteristic energies will certainly lie well above those found here. Trimers are characterized by magnetization plateaux, similar to those of Fig. 3b. However, because of the finite number of spins, they should be in a commensurate relationship with the saturation magnetization and should occur at one-third of this value[35], which is clearly not the case here. Multimers are predicted to occur if there are less than six holes on the chain sublattice[12], as seems to be case (see also Fig. 2c and the Supplementary Methods and discussion therein). However, in the absence of a spectroscopic technique that enables us to reveal the actual form of these excitations we postulate here that the dimers originate from the entanglement of unpaired spins through a chain of local dimers characterized by energy gaps of 100 K, as depicted in Fig. 2c.

The interpretation of our results stems from the natural occurrence of unpaired spins which are periodically arranged in the $Sr_{14}Cu_{24}O_{41}$ lattice. The distance between unpaired spins is calculated to be around $L \approx 8$–9 c-lattice parameters (or, alternatively, $L \approx 220$–250 Å). We could readily calculate the effective exchange between spins, finding $J_{eff} \approx 2.7$–3.1 K, in very good agreement with the value of the spin gap extracted from Fig. 3a,b. By applying an external magnetic field we observe a steep rise of the magnetization and the appearance of up to two

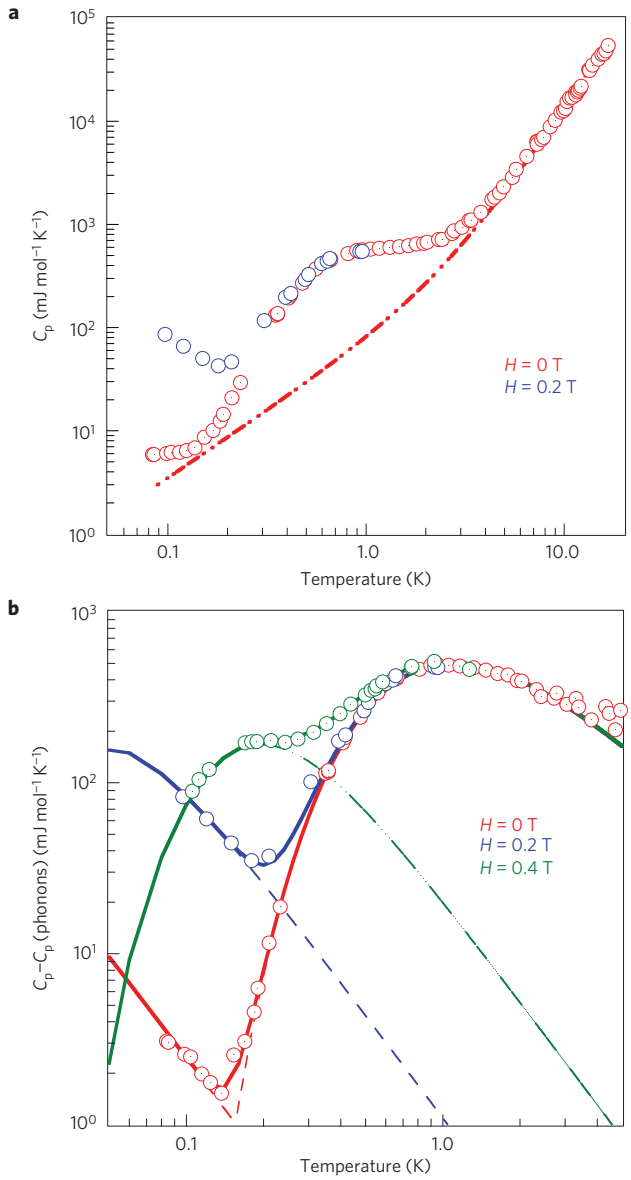

Figure 4 | Low-temperature specific heat experiments at different applied magnetic fields. a, Raw data at nominally 0 T and 0.2 T. Points are the experimental results and the dashed–dotted line is the field-independent component extracted from the results at larger magnetic fields. **b**, Temperature dependence of the magnetic part of the low-temperature specific heat at three magnetic fields. The fit (solid line) was performed with two components. First, a Schottky component (dashed line), $C_P(\theta,\beta) \approx N_{fs}(\theta\beta)^2 e^{-\theta\beta}/(1+e^{-\theta\beta})^2$, with $\theta = 2\mu_B H/k_B$ and $\beta = 1/k_B T$, that accounts for the lowest temperature uprise. This component has no free parameters (Supplementary Methods) and the three magnetic field data were fitted simultaneously. The very small uprise at nominally $H = 0$ T is the signature of a small magnetic field present in our coil that we estimate to be 15 mT. Second, the hump was fitted by $C_P(\beta) \approx (\Delta\beta)^{1.5} \exp(-\Delta\beta)$ and $\Delta = 1.75$ K. This is clearly an approximation, in view of the results of the magnetization experiment, where several components characterized by larger gaps are evident.

magnetization plateaux. Magnetization plateaux can result, for example from frustration, as in the-two dimensional $SrCu_2(BO_3)_2$ (ref. 36), or by intrinsic quantum mechanical effects, as in the double-chains compound NH_4CuCl_3 (ref. 37). Here we believe they are the signature of the disappearance of the spin dimers on forming a ferromagnetic state where the spins are no longer entangled.

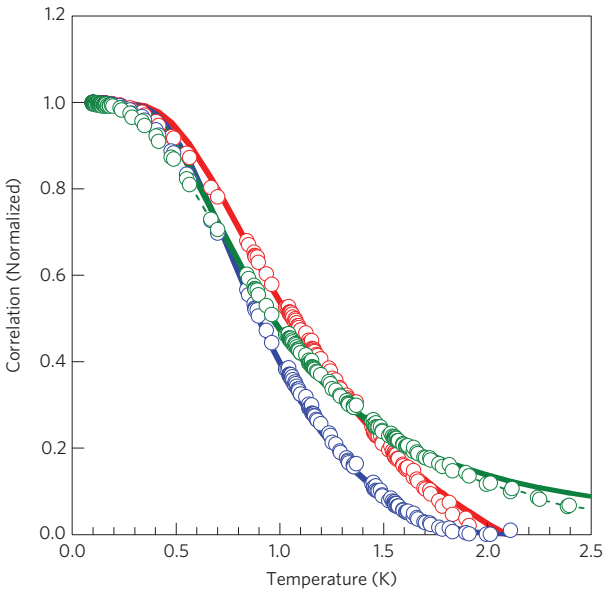

Figure 5 | Quantum correlations. Concurrence (red), entanglement (blue) and quantum information (green) correlations as a function of temperature. Data (in circles) are extracted from Fig. 3a, once the Curie tail has been subtracted. The calculations (solid lines) correspond to the spin-dimer model[21,42].

Whether or not this quantum phase transition is of the form of a Bose–Einstein condensate, as observed in other spin dimers/chains such as $TlCuCl_3$ (ref. 38), $BaCuSi_2O_6$ (refs 39,40), is still a matter of discussion in $Sr_{14}Cu_{24}O_{41}$.

We analysed our data in terms of quantities that characterize the quality of the spin–spin transmission protocol (see Section 3 in Supplementary Methods). Pertinent quantum correlations, such as entanglement, concurrence and quantum discord, have been calculated analytically for the simple Heisenberg spin-dimer Hamiltonian (equation (3); refs 41,42). Concurrence using susceptibility as the entanglement witness is a measure of the ratio of the spin–spin correlation function to the uncorrelated Curie law[17]. Quantum discord has been introduced to account for the total quantumness of the system in the presence of separable (or non-entangled) states[43,44]. Figure 5 shows the variation of concurrence, entanglement and quantum discord correlations as a function of temperature, extracted from the magnetization data (symbols) and the results of the spin-dimer calculation (lines). The calculated quantities based on the spin-dimer model show a remarkable agreement with the experimental data. The entanglement temperature is defined as $T_E \approx \Delta/\log(3) \approx 0.9\Delta \approx 2.1$ K. Transfer fidelity between sites A and B at optimal time for the case $J_p/J_1 = 0.1$ and $T = 100$ mK is of the order of 0.9 (Fig. 4 of ref. 8), much larger than that expected for the maximum classical fidelity, 2/3. Evaluation of quantum discord[45] for the Hamiltonian in (3) yielded identical results to those already found in the literature[42].

Entanglement is ubiquitous in nature provided that the right variables act at the right temperature. $Sr_{14}Cu_{24}O_{41}$ includes up to three types of bipartite spin-1/2 entanglement characterized by maximally entangled states between neighbouring spins. Unpaired spins resulting from the modulation of potentials between two subsystems, chains and ladders[12], ought to entangle at sufficiently low temperatures. Remarkably, owing to the periodicity of the inter-modulation, this mechanism gives rise to the occurrence of unpaired spins at well-defined positions in the chain sublattice. As the characteristic temperatures (and magnetic fields) should be inversely proportional to the distance between unpaired spins, one expects a finite number of these distinctive temperatures. This is the

picture that emerges from our data. It is worth recalling that the picture of well-defined temperatures is expected to disappear in the presence of disorder, as in the $Sr_{14-x}Ca_xCu_{24}O_{41}$ compounds. Strictly speaking, at $T=0$ K there will not be unpaired spins. Consequently, one can expects that the tail observed in magnetization experiments (Fig. 3a) will include those spins that are not yet entangled, in addition to those not arising from a modulation potential. In particular, entanglement between unpaired spins located in adjacent chains (not contemplated in the *ab initio* calculations[12]) should be possible.

Finally, we predict that these dimers could serve as a bus to transmit quantum information at mesoscopic distances in a solid. The mechanism at the origin of unpaired spins in a quantum chain, namely the inter-modulation potential between two sublattices, is amenable to replication. Thin films of a chain-like compound could be grown onto an adequate buffer lattice that can be externally deformed, thus better controlling the distance between spins.

Received 20 June 2014; accepted 10 November 2014; published online 2 February 2015

References

1. Einstein, A., Podolsky, B. & Rosen, N. Can quantum-mechanical description of physical reality be considered complete? *Phys. Rev.* **47,** 777–780 (1935).
2. Nielsen, M. A. & Chuang, I. L. *Quantum Computation and Quantum Information* (Cambridge Univ. Press, 2000).
3. Amico, L., Fazio, R., Osterloh, A. & Vedral, V. Entanglement in many-body systems. *Rev. Mod. Phys.* **80,** 517–576 (2008).
4. Braunstein, S. L. & van Loock, P. Quantum information with continuous variables. *Rev. Mod. Phys.* **77,** 513–577 (2005).
5. Bose, S. Quantum communication through an unmodulated spin chain. *Phys. Rev. Lett.* **91,** 207901 (2003).
6. Bose, S. Quantum communication through spin chain dynamics: An introductory overview. *Contemp. Phys.* **48,** 13–30 (2007).
7. Campos Venuti, L., Degli Esposti Boschi, C. & Roncaglia, M. Long-distance entanglement in spin systems. *Phys. Rev. Lett.* **96,** 247206 (2006).
8. Campos Venuti, L., Degli Esposti Boschi, C. & Roncaglia, M. Qubit teleportation and transfer across antiferromagnetic spin chains. *Phys. Rev. Lett.* **99,** 060401 (2007).
9. Sodano, P., Bayat, A. & Bose, S. Kondo cloud mediated long-range entanglement after local quench in a spin chain. *Phys. Rev. B* **81,** 100412 (2010).
10. Bayat, A., Bose, S. & Sodano, P. Entanglement routers using macroscopic singlets. *Phys. Rev. Lett.* **105,** 187204 (2010).
11. Vuletic, T. *et al.* The spin-ladder and spin-chain system $(La,Y,Sr,Ca)_{14}Cu_{24}O_{41}$: Electronic phases, charge and spin dynamics. *Phys. Rep.* **428,** 169–258 (2006).
12. Gellé, A. & Lepetit, M-B. Influence of the incommensurability in $Sr_{14-x}Ca_xCu_{24}O_{41}$ family compounds. *Phys. Rev. Lett.* **92,** 236402 (2004).
13. Matsuda, M., Yosihama, T., Kakurai, K. & Shirane, G. Quasi-two-dimensional hole ordering and dimerized state in the CuO_2-chain layers in $Sr_{14}Cu_{24}O_{41}$. *Phys. Rev. B* **59,** 1060–1067 (1999).
14. Regnault, L. P. *et al.* Spin dynamics in the magnetic chain arrays of $Sr_{14}Cu_{24}O_{41}$: A neutron inelastic scattering investigation. *Phys. Rev. B* **59,** 1055–1059 (1999).
15. Klingeler, R. *et al.* Magnetization of hole-doped CuO_2 spin chains in $Sr_{14-x}Ca_xCu_{24}O_{41}$. *Phys. Rev. B* **72,** 184406 (2005).
16. Fisher, Daniel S. Random antiferromagnetic quantum spin chains. *Phys. Rev. B* **50,** 3799–3821 (1994).
17. Wiesniak, M., Vedral, V. & Brukner, C. Magnetic susceptibility as a macroscopic entanglement witness. *New J. Phys.* **7,** 258 (2005).
18. Brukner, C., Vedral, V. & Zeilinger, A. Crucial role of quantum entanglement in bulk properties of solids. *Phys. Rev. A* **73,** 012110 (2006).
19. Chakraborty, T., Singh, H., Singh, S., Gopal, R. K. & Mitra, C. Probing quantum discord in a Heisenberg dimer compound. *J. Phys. Condens. Matter* **25,** 425601 (2013).
20. Chakraborty, T. *et al.* Experimental detection of thermal entanglement in a molecular chain. *J. Appl. Phys.* **114,** 144904 (2013).
21. Das, D., Singh, H., Chakraborty, T., Gopal, R. K. & Mitra, C. Experimental detection of quantum information sharing and its quantification in quantum spin systems. *New J. Phys.* **15,** 013047 (2013).
22. Wiesniak, M., Vedral, V. & Brukner, C. Heat capacity as an indicator of entanglement. *Phys. Rev. B* **78,** 064108 (2008).
23. Singh, H. *et al.* Experimental quantification of entanglement through heat capacity. *New J. Phys.* **15,** 113001 (2013).
24. Chakraborty, T., Singh, H. & Mitra, C. Signature of quantum entanglement in $NH_4CuPO_4 \cdot H_2O$. *J. Appl. Phys.* **115,** 034909 (2014).
25. Arnesen, M. C., Bose, S. & Vedral, V. Natural thermal and magnetic entanglement in the 1D Heisenberg model. *Phys. Rev. Lett.* **87,** 017901 (2001).
26. Osborne, Tobias J. & Nielsen, Michael A. Entanglement in a simple quantum phase transition. *Phys. Rev. A* **66,** 032110 (2002).
27. Parmigiani, F. & Sangaletti, L. Behaviour of the Zhang–Rice singlet in $CuGeO_3$, Bi_2CuO_4, and CuO. *J. Electron. Spectrosc. Relat. Phenom.* **107,** 49–62 (2000).
28. Eccleston, R. S. *et al.* Spin dynamics of the spin-ladder dimer-chain material $Sr_{14}Cu_{24}O_{41}$. *Phys. Rev. Lett.* **81,** 1702–1705 (1998).
29. Lorenzo, J. E. *et al.* Macroscopic quantum coherence of the spin triplet in the spin-ladder compound $Sr_{14}Cu_{24}O_{41}$. *Phys. Rev. Lett.* **105,** 097202 (2010).
30. Jolicouer, Th. & Golinelli, O. Sigma-model study of Haldane-gap antiferromagnets. *Phys. Rev. B* **50,** 9265–9273 (1994).
31. Johnston, D. C. *et al.* Thermodynamics of spin $s=1/2$ antiferromagnetic uniform and alternating-exchange Heisenberg chains. *Phys. Rev. B* **61,** 9558–9606 (2000).
32. Kataev, V. *et al.* Interplay of spin and charge dynamics in $Sr_{14-x}Ca_xCu_{24}O_{41}$. *Phys. Rev. B* **64,** 104422 (2001).
33. Klingeler, R. *et al.* Magnetism of hole-doped CuO_2 spin chains in $Sr_{14}Cu_{24}O_{41}$: Experimental and numerical results. *Phys. Rev. B* **73,** 014426 (2006).
34. Hase, M. 1/3 magnetization plateau observed in the $s=1/2$ trimer chain compound $Cu_3(P_2O_6OH)_2$. *Phys. Rev. B* **73,** 104419 (2006).
35. Oshikawa, M., Yamanaka, M. & Affleck, I. Magnetization plateaus in spin chains: Haldane gap for half-integer spins. *Phys. Rev. Lett.* **78,** 1984–1987 (1997).
36. Kageyama, H. *et al.* Exact dimer ground state and quantized magnetization plateaus in the two-dimensional spin system $SrCu_2(BO_3)_2$. *Phys. Rev. Lett.* **82,** 3168–3171 (1999).
37. Shiramura, W. *et al.* Magnetization plateaus in NH_4CuCl_3. *J. Phys. Soc. Jpn* **67,** 1548–1551 (1998).
38. Ruegg, Ch. *et al.* Bose–Einstein condensation of the triplet states in the magnetic insulator $TlCuCl_3$. *Nature* **423,** 62–65 (2003).
39. Jaime, M. *et al.* Magnetic-field-induced condensation of triplons in Han purple pigment. *Phys. Rev. Lett.* **93,** 087203 (2004).
40. Sebastian, S. E. *et al.* Dimensional reduction at a quantum critical point. *Nature* **441,** 617–620 (2006).
41. Modi, K., Brodutch, A., Cable, H., Paterek, T. & Vedral, V. The classical-quantum boundary for correlations: Discord and related measures. *Rev. Mod. Phys.* **84,** 1655–1707 (2012).
42. Aldoshin, S. M., Fel'dman, E. B. & Yurishchev, M. A. Quantum entanglement and quantum discord in magnetoactive materials. *Low Temp. Phys.* **40,** 1–16 (2014).
43. Henderson, L. & Vedral, V. Classical, quantum and total correlations. *J. Phys. A* **34,** 6899–6905 (2001).
44. Ollivier, H. & Zurek, W. H. Quantum discord: A measure of the quantumness of correlations. *Phys. Rev. Lett.* **88,** 017901 (2001).
45. Luo, S. Quantum discord for two-qubit systems. *Phys. Rev. A* **77,** 042303 (2008).

Acknowledgements

We acknowledge the support of the European Community Research Infrastructures under the FP7 Capacities Specific Program, MICROKELVIN project number 228464.

Author contributions

The idea was born out of discussion between J.E.L. and S.S. Samples came from V.S., C.M. and A.R. The magnetization experiment was carried out by C.P., the specific heat experiment was carried out by G.R. and S.S. and the inelastic-neutron-scattering experiment was carried out on the three-axis spectrometer IN12 at ILL, Grenoble, by J.E.L., L.P.R. and S.R. The data were analysed by S.S. and J.E.L. Finally J.E.L. wrote the manuscript with input from all the authors.

Additional information

Supplementary information is available in the online version of the paper. Reprints and permissions information is available online at www.nature.com/reprints. Correspondence and requests for materials should be addressed to J.E.L.

Competing financial interests

The authors declare no competing financial interests.